

Fast AI Model Splitting over Edge Networks

Zuguang Li, *Graduate Student Member, IEEE*, Wen Wu *Senior Member, IEEE*, Shaohua Wu *Member, IEEE*, Songge Zhang, Ye Wang, *Member, IEEE*, and Xuemin (Sherman) Shen *Fellow, IEEE*

Abstract—Split learning (SL) has emerged as a computationally efficient approach for artificial intelligence (AI) model training, which can alleviate device-side computational workloads. However, complex AI model architectures pose a high computational complexity to obtain the optimal model splitting. In this paper, we represent an arbitrary AI model as a directed acyclic graph (DAG), and then reformulate the optimal model splitting problem as a minimum s - t cut search problem. To solve the problem, we propose a fast DAG-based model splitting algorithm, which restructures the DAG to enable the optimal model splitting identification via a maximum flow method. Theoretical analysis indicates that the proposed algorithm is optimal. Furthermore, considering AI models with block structures, we propose a block-wise model splitting algorithm to reduce computational complexity. The algorithm abstracts each block, i.e., a component consisting of multiple layers, into a single vertex, thereby obtaining the optimal model splitting via a simplified DAG. Extensive experimental results demonstrate that the proposed algorithms can determine the optimal model splitting within milliseconds, as well as reduce training delay by 24.62%–38.95% in dynamic edge networks as compared to the state-of-the-art benchmarks.

Index Terms—Split learning, fast model splitting, block-wise, directed acyclic graph.

I. INTRODUCTION

Artificial intelligence (AI) is expected to be natively integrated into the next generation networks, thereby enabling a wide variety of intelligent services such as healthcare, autonomous driving, and smart city. In turn, the massive data generated by distributed devices in the next generation networks can enhance the performance of AI models [1]. These devices are often unwilling to share the data they collect due to privacy concerns [2]. Federated learning (FL) has been proposed to facilitate collaborative model training without sharing raw data [3]. However, FL performs the entire model training on devices, which imposes a significant computational workload on resource-constrained devices.

Split learning (SL), as a promising distributed learning framework, has been proposed to address the weakness of FL [4]. Specially, SL divides a global AI model into device-side and a server-side models. Each device trains only its

device-side model using its own data and transmits small-scale intermediate results (i.e., smashed data and gradients) instead of raw data to the server [5]. Therefore, SL can offload the computational workload from devices to a server while allowing the devices to retain their raw data. In SL, the model splitting (i.e., the cut layer selection) is essential, especially for edge networks, since it directly affects both the communication overhead and device-side computational workloads.

In the literature, several model splitting methods have been proposed for SL to accelerate AI model training. A brute-force search method was used to find the optimal cut layer that minimizes model training latency [6]. A regression-based method was designed to quantify the relationships between the cut layer and both the communication overhead and computational workload, enabling the optimal cut layer to be obtained by solving an optimization problem [7]. In addition, an approximate model splitting algorithm was proposed to determine the optimal cut layer, thereby minimizing the inference delay [8]. However, the regression and approximate model splitting methods only work for linear AI models and the chosen cut layer is suboptimal. Although the brute-force search method can theoretically find the optimal cut layer, its prohibitive computational complexity makes it infeasible for complex models. Therefore, can we develop an efficient and generalizable approach to determine the optimal model splitting for arbitrary AI architectures?

In this paper, we investigate the model splitting problem for SL, aiming to fast determine the optimal model splitting that minimizes training delay in edge networks. To achieve this goal, *firstly*, we represent an AI model as a directed acyclic graph (DAG) to reformulate the optimal model splitting problem as a minimum s - t cut search problem. Specially, the AI model's layers are represented as vertices and the connections between layers are represented as edges. To directly encode the computation and transmission delays into the DAG, we define three types of edge weights. *Secondly*, to solve the minimum s - t cut search problem, we propose a DAG-based model splitting algorithm, which restructures the DAG by adding an auxiliary vertex for each parent vertex with multiple child vertices. The minimum s - t cut can be then obtained by a maximum flow method. We further prove that the cut obtained by the DAG-based model splitting algorithm is optimal. *Thirdly*, considering AI models with block structures, we propose a block-wise model splitting algorithm to reduce the computational complexity. The algorithm leverages an intra-block cut detection based only on smashed data size to determine whether the minimum s - t cut intersects intra-block edges. Each block, i.e., a component consisting of multiple layers, is abstracted into a single vertex when the minimum s - t cut is identified not to intersect any intra-block

Zuguang Li is with School of Electronics and Information Engineering, Harbin Institute of Technology, Shenzhen 518055, China, and also with the Frontier Research Center, Pengcheng Laboratory, Shenzhen, 518055, China (e-mail: lizg01@pcl.ac.cn).

Wen Wu, Songge Zhang, and Ye Wang are with the Pengcheng Laboratory, Shenzhen, 518055, China (e-mails: {wuw02, zhangsg, wangy02}@pcl.ac.cn).

Shaohua Wu is with Harbin Institute of Technology, Shenzhen 518055, China, and also with Department of Broadband Communication, Pengcheng Laboratory, Shenzhen, 518055, China (e-mail: hitwush@hit.edu.cn).

Xuemin (Sherman) Shen is with the Department of Electrical and Computer Engineering, University of Waterloo, Waterloo, ON N2L 3G1, Canada (email: sshen@uwaterloo.ca).

This paper has been submitted to the *IEEE Journal on Selected Areas in Communications* for review.

edges. The optimal model splitting can be then determined efficiently in a simplified DAG. Our experimental results based on a physical platform with several NVIDIA Jetson devices demonstrate that: (i) the proposed solution can determine the optimal model splitting for SL within milliseconds, reducing the running time by up to 13.0 \times compared to the baselines; and (ii) the proposed solution accelerates model training, reducing the overall training delay by up to 38.95% compared to the baselines. The main contributions of this work are summarized as follows.

- We represent an arbitrary AI model as a general DAG, and then convert the optimal model splitting problem as a minimum s - t cut search problem.
- We propose a DAG-based model splitting algorithm to determine the optimal cut and prove its optimality.
- We propose a block-wise model splitting algorithm for AI models with blocks, which can further reduce computational complexity.

The remainder of this paper is organized as follows. Section II reviews related works, followed by the system model in Section III. The DAG representing of AI models is presented in Section IV. The DAG-based and block-wise model splitting algorithm are presented in Sections V and VI, respectively. Performance evaluation is provided in Section VII. Finally, Section VIII concludes this paper.

II. RELATED WORK

Split learning has attracted widespread attention and investigation. In the 3rd generation partnership project (3GPP) Release 18, the performance advantages of AI model splitting has been recognized and protocol-level primitives have been explored to support model splitting between end devices and the server [9]. A communication-aware SL framework with an early-exit mechanism was developed to accommodate devices with diverse computational capabilities and fluctuating channel conditions [10]. An online model splitting strategy was proposed to minimize energy and latency costs under dynamic wireless channel conditions [11]. To support dynamic networks, a cluster-based outgoing SL framework was introduced, enabling a first-outgoing-then-sequential training paradigm for heterogeneous devices [12]. Similarly, a parallel SL framework was proposed where all devices collaboratively train the device-side model with the server, addressing computational heterogeneity in edge networks [6]. To further improve communication efficiency, a split federated learning framework was designed, where cut selection and bandwidth allocation are jointly optimized to minimize overall system latency [13]. The existing works have explored SL to address challenges such as heterogeneous computing capabilities and dynamic channel conditions in edge networks. Differently, our work focuses on the optimal model splitting in SL to reduce the computational complexity of the cut layer selection algorithm and the overall training delay.

The cut layer selection of SL directly impacts computational workload and communication overload. A theoretical analysis of split federated learning was conducted to examine how the cut layer selection influences convergence and overall performance [14]. Another study modeled the cut layer selection

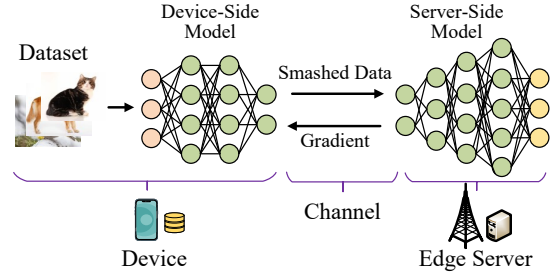


Fig. 1: Considered wireless SL scenario in edge networks.

process as a Stackelberg game to optimize client incentives and data contributions while balancing privacy preservation and energy consumption [15]. To determine the optimal cut layer, various approaches have been proposed, including brute-force search [6], binary search [16], regression-based search [7], and graph-based search approaches [17]–[19]. A brute-force search method was proposed to identify the optimal cut layer for either minimum latency or mobile energy consumption, based on profiling per-layer execution time and energy usage across different AI models [20]. A binary search-based splitting algorithm was designed for pipeline inference in line-structured models [16]. In graph-based approaches, one DAG-based approach was proposed to select the optimal cut layer under dynamic network conditions, therefore reducing inference latency in edge–cloud systems [17]. Another approach addressed multi-partitioning in DAG-topology networks through graph transformation and partitioning techniques [19]. The existing cut layer selection approaches are primarily designed for linear AI models, limiting their applicability to more complex architectures. Differently, our work focuses on finding the optimal model splitting for arbitrary AI models, including both linear and nonlinear structures.

III. SYSTEM MODEL

A. Considered Scenario

In this subsection, we present a typical SL scenario in an edge network and the model training process. As shown in Fig. 1, the system includes mobile devices and an edge server. The AI model is split between the device and server, with intermediate data transmitted via wireless channels. Key system components are described as follows:

- *Edge server:* The edge server is equipped with a base station that can perform server-side model training. Moreover, it is responsible for collecting network information, such as device computing capabilities and channel conditions, to make decisions on cut selection.
- *Devices:* The devices are endowed with computing capabilities, which can perform device-side model training. They have local datasets and corresponding labels for model training.

Considering the heterogeneous device capabilities and the dynamic channel conditions in edge networks, the server dynamically determine the optimal cut for each device in every training epoch. Before training begins, the model parameters are randomly initialized. In each training epoch, the server

collects device and network information, and selects a device for training in a round-robin manner. Based on the information, the server determines the model splitting, denoted by $c = \{\mathcal{V}_D, \mathcal{V}_S\}$, where \mathcal{V}_D and \mathcal{V}_S denote the sets of layers assigned to the device and server, respectively. The device and server then jointly train the model over N local iterations.

During each local iteration, the device performs forward propagation on the device-side model and transmits the smashed data and corresponding labels to the server. The server completes forward and backward propagation on the server-side model and returns the gradients to the device, which subsequently updates its device-side model. After completing local iterations, the device uploads its updated device-side model to the server, which integrates the updates and distributes the updated device-side model to the next selected device. This process is repeated across devices over multiple training epochs until the global model converges.

B. Training Delay

In SL, the computation and transmission delays are analyzed as follows.

1) *Computation Delay*: During each training epoch, the device-side model and the server-side model are trained at the device and server, respectively, whose delays are analyzed as follows:

- *Device-side model computation delay*: The computation delay in processing layer v_i is defined as ξ_{D,v_i} . Note that ξ_{D,v_i} consists of the forward and backward propagation computation delay at layer v_i . The device-side model computation delay can be defined as

$$T_{D,C} = \sum_{v_i \in \mathcal{V}_D} \xi_{D,v_i}. \quad (1)$$

- *Server-side model computation delay*: For the server, the computation delay in processing layer v_i is defined as ξ_{S,v_i} . Hence, its computation delay can be defined as

$$T_{S,C} = \sum_{v_i \in \mathcal{V}_S} \xi_{S,v_i}. \quad (2)$$

2) *Transmission Delay*: During SL, the device-side model, smashed data, and its gradients, are exchanged between the device and server, incurring transmission delay. The detailed analysis is as follows.

- *Device-side model downloading delay*: Let R_S denote the transmission rate from the server to the device, and k_{v_i} denote the data size of the parameters in layer v_i . Hence, the downloading delay for transmitting the device-side model can be defined as

$$T_{S,D} = \frac{\sum_{v_i \in \mathcal{V}_D} k_{v_i}}{R_S}. \quad (3)$$

- *Smashed data transmission delay*: Let R_D denote the average transmission rate from the device to the server, and a_{v_i} denote the data size of the smashed data of vertex v_i in the forward propagation. The transmission delay for transmitting the smashed data can be defined as

$$T_{D,S} = \frac{\sum_{v_i \in \mathcal{V}_c} a_{v_i}}{R_D}, \quad (4)$$

where \mathcal{V}_c is the sets of end layers on the device-side model after the AI model is split by the cut.

- *Smashed data's gradient transmission delay*: Let \tilde{a}_{v_i} denote the size of the smashed data's gradient received by vertex v_i during backward propagation. During AI model training, the size of smashed data is equal to that of its corresponding gradient, i.e., $\tilde{a}_{v_i} = a_{v_i}$. The transmission delay for transmitting the gradient can be defined as

$$T_{S,G} = \frac{\sum_{v_i \in \mathcal{V}_c} \tilde{a}_{v_i}}{R_S}. \quad (5)$$

- *Device-side model uploading delay*: The device-side model uploading delay can be defined as

$$T_{D,U} = \frac{\sum_{v_i \in \mathcal{V}_D} k_{v_i}}{R_D}. \quad (6)$$

3) *Overall Model Training Delay*: Taking all the computation and transmission delay components into account, the model training delay is given by

$$T(c) = N (T_{D,C} + T_{D,S} + T_{S,C} + T_{S,G}) + T_{D,U} + T_{S,D}. \quad (7)$$

Our goal is to find the optimal model splitting that minimizes the overall training delay, i.e., $\min T(c)$. However, solving this optimization problem is challenging, especially when the AI model exhibits a complex nonlinear structure. In the next section, we transform the AI model into a DAG, where edge weights explicitly reflect these delays.

IV. DAG REPRESENTING OF AI MODELS

In this section, we represent an AI model as a DAG, with edge weights encoding the computation and transmission delays. Based on this DAG, we formulate the optimal model splitting problem as a minimum s - t cut problem.

A. DAG Model

1) *DAG Construction*: As illustrated in Fig. 2(a), a typical AI model consists of various types of layers, such as convolutional layers, pooling layers, and fully connected layers. These layers are connected via data dependencies, forming a computational graph. This graph can be represented as a DAG, as shown in Fig. 2(b). The DAG is defined as

$$\mathcal{G} = (\mathcal{V} \cup \{D, S\}, \mathcal{E}). \quad (8)$$

Here, $\mathcal{V} = v_1, v_2, \dots, v_L$ denotes the set of layer vertices, where each vertex v_i corresponds to a specific layer in the AI model, and L is the total number of layers. To represent the computation flow from device to server, we introduce two virtual vertices: D , *source vertex*, representing a virtual device, and S , *sink vertex*, representing a virtual server. Let \mathcal{E} be the set of directed edges, where each edge $(v_i, v_j) \in \mathcal{E}$ indicates that the output of layer v_i is used as the input to layer v_j in the AI model. Therefore, the AI model structure can be represented as a DAG. In addition, we add edges from the source vertex D to each layer vertex $v_i \in \mathcal{V}$, and from each layer vertex $v_i \in \mathcal{V}$ to the sink vertex S , so that the entire AI model is enclosed between the source and sink vertices.

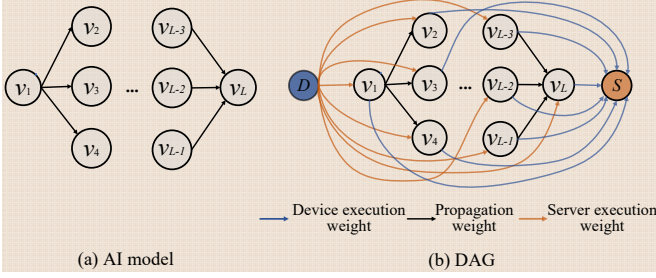


Fig. 2: Illustration of representing an AI model as a DAG. (a) The AI model consists of multiple layers. (b) The corresponding DAG adds a source and a sink vertex.

2) *Mapping Delay into DAG*: The main challenge in using DAG for solving the optimal model splitting problem is that it cannot directly represent the computation delay, device-side model uploading delay, or device-side model downloading delay through vertex or edge weights. This is because the computation delay of each layer depends on whether it is executed on the device or the server, while the uploading and downloading delays depend on the specific subset of layers trained on the device. To address this, the model training delays (including the computation delay and transmission delay) are mapped into three types of edge weights in the DAG as follows:

- *Device execution weight*: The weight of the directed edge from each layer vertex $v_i \in \mathcal{V}$ to the sink vertex S represents the device execution weight when v_i is executed on the device. This weight is defined as the sum of the computation delay for training v_i on the device and the transmission delay for uploading v_i during the device-side model update. It is calculated as

$$w_{(D,v_i)} = N\xi_{D,v_i} + \frac{k_{v_i}}{R_D}. \quad (9)$$

- *Server execution weight*: The weight of the directed edge from source vertex D to each layer vertex $v_i \in \mathcal{V}$ represents the server execution weight when v_i is executed on the server. This weight is defined as the sum of the computation delay for training v_i on the server and the transmission delay for downloading v_i during the device-side model distribution. It is calculated as

$$w_{(v_i,S)} = N\xi_{S,v_i} + \frac{k_{v_i}}{R_S}. \quad (10)$$

- *Propagation weight*: The weight of the directed edge between any two layer vertices $v_i, v_j \in \mathcal{V}$ represents the propagation weight. This weight is defined as the sum of the transmission delay of v_i 's smashed data during forward propagation and v_j 's gradient during backward propagation. It is calculated as

$$w_{(v_i,v_j)} = N \left(\frac{a_{v_i}}{R_D} + \frac{\tilde{a}_{v_i}}{R_S} \right). \quad (11)$$

Here, \tilde{a}_{v_i} denotes the size of the gradient received by vertex v_i from v_j during backward propagation, which equals the size of the smashed data in forward propagation, i.e., $\tilde{a}_{v_i} = a_{v_i}$.

Algorithm 1: DAG Building Process.

```

1 Build  $\mathcal{G} = (\mathcal{V} \cup \{D, S\}, \mathcal{E})$  based on the AI model
  structure;
2 for each  $v_i \in \mathcal{V}$  do
3   | Add edges  $(D, v_i)$  and  $(v_i, S)$  to  $\mathcal{E}$ ;
4 end
5 for each  $(v_i, v_j) \in \mathcal{E}$  do
6   | if  $v_i == D$  then
7     | Calculate  $w_{(v_i,v_j)}$  based on Eq. (9);
8   | else if  $v_j == S$  then
9     | Calculate  $w_{(v_i,v_j)}$  based on Eq. (10);
10  | else
11    | Calculate  $w_{(v_i,v_j)}$  based on Eq. (11);
12  | end
13  | Assign  $w_{(v_i,v_j)}$  to edge  $(v_i, v_j)$ ;
14 end

```

Through the above process, the computation and transmission delays are encoded as the weights of the edges in DAG \mathcal{G} . As shown in Fig. 2(b), the edges with device execution, server execution, and propagation weights are colored blue, orange, and black respectively. The detailed procedure for constructing the DAG from an AI model is presented in Alg. 1. Note that in the DAG, the vertices themselves are unweighted and serve only to represent the AI model layers, the virtual device, and the virtual server.

B. Problem Formulation

We aim to minimize the overall training delay in SL, which can be reformulated as a minimum s - t cut problem in the DAG, i.e., finding an s - t cut that minimizes the total weight of the edges intersected by the cut. An s - t cut partitions the vertex set into two disjoint subsets \mathcal{V}_D and \mathcal{V}_S , such that the source vertex $D \in \mathcal{V}_D$ and the sink vertex $S \in \mathcal{V}_S$. The value of an s - t cut $c = \{\mathcal{V}_D, \mathcal{V}_S\}$ is defined as the sum of the weights of all edges directed from \mathcal{V}_D to \mathcal{V}_S . Let $\mathcal{W}(c)$ denote the set of weights of these edges, then the value of the cut can be expressed as $T_{\mathcal{G}}(c) = \sum_{w \in \mathcal{W}(c)} w$. Thus, the minimum s - t cut problem in the DAG can be formulated as follows:

$$\begin{aligned}
& \min_c T_{\mathcal{G}}(c) \\
& \text{s.t. } c \in \mathcal{C}, \\
& \quad D \in \mathcal{V}_D, \\
& \quad S \in \mathcal{V}_S.
\end{aligned} \quad (12)$$

Here, \mathcal{C} is a set of all available cuts in the DAG and the first constraint guarantees the feasibility of the cut selection. The second and third constraints ensure that the source vertex is placed on the device, while the sink vertex is placed on the server, respectively.

This problem cannot be directly solved using standard minimum s - t cut algorithms when the AI model is nonlinear. In such models, if the cut intersects multiple outgoing edges from the same parent vertex, the corresponding propagation weight may be counted multiple times in the DAG, leading

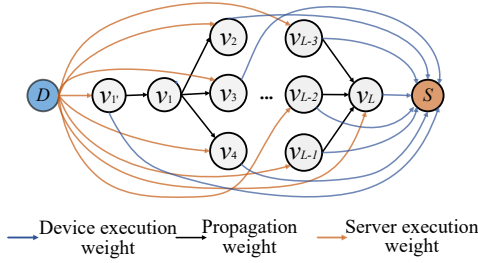


Fig. 3: Illustration of adding an auxiliary vertex for a parent vertex with multiple child vertices.

to an overestimated cut value. However, in the actual AI model, the smashed data and its corresponding gradient from a parent vertex only need to be transmitted once, regardless of how many outgoing edges it has. To address this issue, we introduce a DAG-based model splitting algorithm in the following section.

V. DAG-BASED MODEL SPLITTING ALGORITHM

In this section, we propose the DAG-based model splitting algorithm to determine the optimal model splitting for an arbitrary AI model architecture. We also prove that the cut obtained by this algorithm is optimal.

A. Algorithm Design

To eliminate the overestimation of propagation weights in nonlinear DAGs, we introduce a DAG-based model splitting algorithm. This algorithm restructures the DAG to prevent duplicated counting of transmission weights from the same parent vertex. The main steps are described as follows.

- 1) Initialize a DAG $\mathcal{G}' = (\mathcal{V}' \cup \{D, S\}, \mathcal{E}')$ by setting $\mathcal{V}' = \mathcal{V}$ and $\mathcal{E}' = \mathcal{E}$. Then, identify the set of parent vertices that have multiple child vertices in \mathcal{G}' , denoted as $\mathcal{V}_{\mathcal{P}}$.
- 2) For each parent vertex $v_p \in \mathcal{V}_{\mathcal{P}}$, an auxiliary vertex $v_{p'}$ is introduced into the DAG, as illustrated in Fig. 3.
- 3) All incoming edges originally connected to v_p are redirected to the new vertex $v_{p'}$, while preserving their original weights:

$$w_{(v_i, v_{p'})} = w_{(v_i, v_p)}, \quad (13)$$

where v_i is a parent of v_p . For example, in Fig. 3, edge (v_D, v_1) becomes $(v_D, v_{1'})$, satisfying $w_{(v_D, v_{1'})} = w_{(v_D, v_1)}$.

- 4) The edge from v_p to the sink vertex S is also redirected to originate from $v_{p'}$, with its weight unchanged:

$$w_{(v_{p'}, S)} = w_{(v_p, S)}. \quad (14)$$

As shown in Fig. 3, edge (v_1, v_S) becomes $(v_{1'}, v_S)$, and we have $w_{(v_{1'}, v_S)} = w_{(v_1, v_S)}$.

- 5) Add a new edge from the auxiliary vertex to the original parent vertex, i.e., $(v_{p'}, v_p)$, with a weight equal to the propagation cost from v_p to one of its child vertices:

$$w_{(v_{p'}, v_p)} = w_{(v_p, v_j)}, \quad (15)$$

Algorithm 2: DAG-Based Model Splitting Algorithm.

- 1 Build a DAG \mathcal{G} for an AI model based on Alg. 1;
- 2 Find out the set $\mathcal{V}_{\mathcal{P}}$ of parent vertices with several child vertices;
- 3 **if** $\mathcal{V}_{\mathcal{P}} = \emptyset$ **then**
- 4 Obtain minimum s - t cut $c_{\mathcal{G}}^*$ of \mathcal{G} via the brute-force search;
- 5 $c^* = c_{\mathcal{G}}^*$;
- 6 **else**
- 7 $\mathcal{E}' \leftarrow \mathcal{E}$, $\mathcal{V}' \leftarrow \mathcal{V}$;
- 8 **for** v_p **in** $\mathcal{V}_{\mathcal{P}}$ **do**
- 9 Add auxiliary vertex $v_{p'}$ to \mathcal{V}' ;
- 10 The edges pointing to parent vertex v_p are migrated from v_p to $v_{p'}$;
- 11 Calculate $w_{(v_i, v_{p'})}$ based on Eq. (13);
- 12 Assign $w_{(v_i, v_{p'})}$ to edge $(v_i, v_{p'})$ in \mathcal{G}' ;
- 13 The edge between v_p and S are migrated from v_p to $v_{p'}$;
- 14 Calculate $w_{(v_{p'}, S)}$ based on Eq. (14);
- 15 Assign $w_{(v_{p'}, S)}$ to edge $(v_{p'}, S)$ in \mathcal{G}' ;
- 16 Add an edge $(v_{p'}, v_p)$ to \mathcal{E}' ;
- 17 Calculate $w_{(v_{p'}, v_p)}$ based on Eq. (15);
- 18 Assign $w_{(v_{p'}, v_p)}$ to edge $(v_{p'}, v_p)$ in \mathcal{G}' ;
- 19 **end**
- 20 $\mathcal{G}' = (\mathcal{V}' \cup \{D, S\}, \mathcal{E}')$;
- 21 Obtain minimum s - t cut $c_{\mathcal{G}'}^*$ of \mathcal{G}' via the maximum flow method;
- 22 $c^* = c_{\mathcal{G}'}^*$;
- 23 **end**
- 24 **return** Optimal cut c^* .

where v_j is a child of v_p . For example, in Fig. 3, edge $(v_{1'}, v_1)$ is added with $w_{(v_{1'}, v_1)} = w_{(v_1, v_2)}$.

After the above process, we build a new DAG \mathcal{G}' for nonlinear AI models. This new DAG resolves the issue of counting the same propagation weight multiple times when a cut intersects multiple edges from the same parent vertex. The optimal cut can then be obtained by solving the minimum s - t cut problem on \mathcal{G}' , which can be efficiently solved using standard maximum-flow algorithms, such as Dinic's algorithm [21]. For linear AI models, this issue does not exist, as each layer has at most one child. Thus, the optimal cut can be directly computed on the original DAG \mathcal{G} using simple algorithms such as the brute-force search method. The detailed procedure of the DAG-based model splitting algorithm is presented in Alg. 2.

B. Performance Analysis

For linear AI models, it is straightforward to see that the minimum s - t cut in the DAG is exactly equivalent to the optimal cut layer in the AI model. Therefore, in this subsection, we focus on proving the equivalence between the optimal cut in nonlinear AI models and the minimum s - t cut in the DAG \mathcal{G}' . To prove this equivalence, it begins with the following reasonable assumption.

Assumption 1. *The server's computing capability is at least as strong as the device's. Specifically, for any layer, the computation latency on the server is no greater than that on the device, i.e.,*

$$\xi_{D,v_i} - \xi_{S,v_i} \geq 0, \forall v_i \in \mathcal{V}. \quad (16)$$

Under Assumption 1, we can rigorously prove that minimizing the training delay in the AI model is equivalent to finding the minimum s - t cut in the corresponding DAG. This relationship is formalized in the following theorem.

Theorem 1. *The minimum s - t cut in the DAG \mathcal{G}' corresponds exactly to the optimal cut that minimizes the training delay in the AI model.*

Proof. As shown in Fig. 4, all possible cuts in an AI model can be categorized into three cases: (i) the cut intersects all outgoing edges originating from a parent vertex, e.g., case 1 in Fig. 4(a); (ii) the cut intersects only some of the outgoing edges from a parent vertex, e.g., case 2 in Fig. 4(b); and (iii) the cut does not intersect any outgoing edges from a parent vertex, e.g., case 3 in Fig. 4(c). Let $T(\cdot)$ denote the model training delay in the original AI model, calculated as the sum of computation and transmission delays. Let $T_{\mathcal{G}'}(\cdot)$ denote the value of the s - t cut in DAG \mathcal{G}' , calculated as the sum of the weights of all edges intersected by this cut. The corresponding training delay under each case is analyzed as follows.

- Case 1: The model training delay in the AI model is equal to the value of the cut crossing the edge from the auxiliary vertex to its original vertex in \mathcal{G}' . For example, the value of cut c_1 in Fig. 4(a) is the same as that of cut $c_{1'}$ in Fig. 5(a), i.e., $T(c_1) = T_{\mathcal{G}'}(c_{1'})$. In addition, the original cut in \mathcal{G}' (e.g., cut c_1 in Fig. 5(a)) is impossible to be the minimum s - t cut, because its value is more than the value of the cut crossing the edge between the auxiliary vertex and its original vertex (e.g., $T_{\mathcal{G}'}(c_{1'}) < T_{\mathcal{G}'}(c_1)$ in Fig. 5(a)). In cut c_1 of Fig. 5(a), the weights of outgoing edges from vertex v_1 are counted three times, while the weight of the outgoing edge from vertex $v_{1'}$ is counted only once in cut $c_{1'}$. This leads to $T_{\mathcal{G}'}(c_{1'}) < T_{\mathcal{G}'}(c_1)$. Hence, this case does not require further analysis.
- Case 2: If the server's computing capability is not weaker than that of the device, the corresponding model training delay in the AI model cannot be minimal, and the cut in this case cannot be the minimum s - t cut in \mathcal{G}' . We first analyze the cut in the AI model. Compared with *case 1*, the model training delay in *case 2* is strictly larger. For instance, as shown in Fig. 4(a) and Fig. 4(b), the difference in delay between cut c_2 and cut c_1 is given by

$$T(c_2) - T(c_1) = N \left(\xi_{D,v_4} - \xi_{S,v_4} + \frac{a_{v_4}}{R_D} + \frac{a_{v_4}}{R_S} \right) + \frac{k_{v_4}}{R_D} + \frac{k_{v_4}}{R_S}. \quad (17)$$

Under Assumption 1, we have $\xi_{D,v_4} - \xi_{S,v_4} \geq 0$, which leads to $T(c_2) - T(c_1) > 0$. Therefore, the cut in *case 2* cannot be the optimal cut in the AI model.

We then examine the corresponding cut in the DAG \mathcal{G}' and find that the same conclusion holds, i.e., the cut in

case 2 is not the minimum s - t cut in \mathcal{G}' . For example, as illustrated in Fig. 5(a) and Fig. 5(b), the difference in cut values is

$$T_{\mathcal{G}'}(c_2) - T_{\mathcal{G}'}(c_1) = N \left(\xi_{D,v_4} - \xi_{S,v_4} + \frac{a_{v_1}}{R_D} + \frac{a_{v_1}}{R_S} + \frac{a_{v_4}}{R_D} + \frac{a_{v_4}}{R_S} \right) + \frac{k_{v_4}}{R_D} + \frac{k_{v_4}}{R_S}. \quad (18)$$

Given Assumption 1, we again have $T_{\mathcal{G}'}(c_2) - T_{\mathcal{G}'}(c_1) > 0$, confirming that the cut in *case 2* cannot be the minimum s - t cut in \mathcal{G}' .

- Case 3: The model training delay in the AI model is precisely equal to the value of the corresponding cut in \mathcal{G}' . For example, the value of cut c_3 in Fig. 4(c) matches that of cut c_3 in Fig. 5(c), i.e., $T(c_3) = T_{\mathcal{G}'}(c_3)$. Since this case exhibits a one-to-one correspondence between the training delay and the cut value, no further analysis is necessary.

In summary, based on the analysis of all three cases, we have completed the proof. \square

VI. BLOCK-WISE MODEL SPLITTING ALGORITHM

In this section, we present the block-wise model splitting algorithm to determine the optimal model splitting for AI models with block structures.

A. Intra-Block Cut Identification

The DAG-based model splitting algorithm proposed in the previous section can determine the optimal cut for arbitrary AI models. However, when an AI model contains structural patterns, referred to as blocks, there is an opportunity to further reduce the computational complexity of the cut selection process. A block is defined as a group of layers with shared internal structure and transformation logic, often reused multiple times within the model. For example, the inception block is reused 9 times in GoogLeNet [22], the residual block is reused 8 and 16 times in ResNet18 and ResNet50 [23], respectively, and the dense block is reused 58 and 98 times in DenseNet121 and DenseNet201 [24], respectively. These blocks share the same internal architecture and transformation logic, although their input and output dimensions may vary depending on their position in the model. Because of this structural repetition, analyzing a representative block allows us to generalize its behavior across the other same blocks.

To reduce the complexity of cut computation, we perform an intra-block cut identification to determine whether the optimal cut intersects the internal edges of any block. This identification only relies on the sizes of smashed data within the block and does not require device or network parameters. If the optimal cut intersects a block's internal edges, the block must be preserved in full. Otherwise, it can be safely abstracted as a single vertex of the DAG, simplifying the DAG structure and accelerating the cut selection process.

A block DAG is denoted by $\mathcal{G}_B = (\mathcal{V}_B, \mathcal{E}_B)$, where each vertex in \mathcal{V}_B represents a layer within the block and each directed edge in \mathcal{E}_B indicates the flow of smashed data

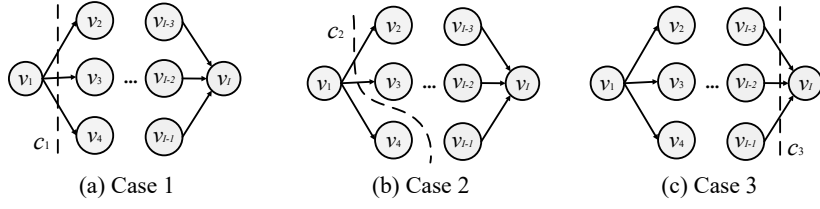


Fig. 4: Three cut cases in the AI model, where each cut's value is the total training delay.

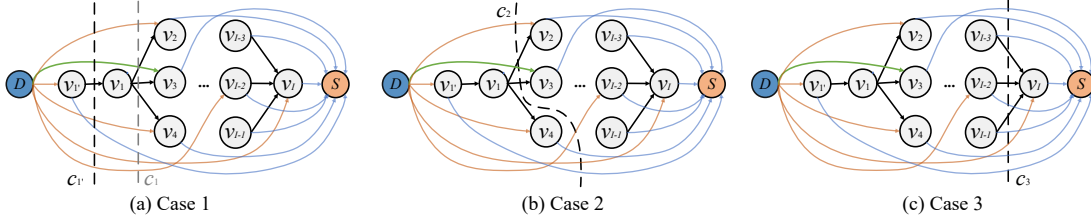


Fig. 5: Three cut cases in the DAG, where each cut's value is the sum of the weights of the edges that the cut intersects.

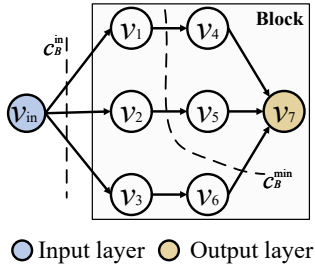


Fig. 6: An example block DAG, with edge weights representing the size of smashed data.

between layers. The input layer of the block is denoted as vertex v_{in} . As shown in Fig. 6, $\mathcal{V}_B = \{v_1, \dots, v_7\}$ and v_{in} is the input layer. The vertices are unweighted, and each edge is weighted by the size of the smashed data from its parent vertex. The input and output layers of the block are treated as the source and sink of \mathcal{G}_B , respectively. Let c_B^{in} be the cut that separates the input layer from this block, with a corresponding cut value a_B^{in} , which equals the size of the smashed data from the input vertex v_{in} . Let c_B^{min} denote the minimum $s-t$ cut of the block, and a_B^{min} be its cut value, which can be computed using standard minimum $s-t$ cut algorithms [21], [25]. If $a_B^{min} \geq a_B^{in}$, the optimal cut does not intersect any intra-block edges. Otherwise, it may intersect the intra-block edges.

Under Assumption 1, we derive the following theorem about the optimal cut:

Theorem 2. *If $a_B^{min} \geq a_B^{in}$, the optimal cut does not intersect any intra-block edges.*

Proof. Please refer to Appendix A. \square

If $a_B^{min} < a_B^{in}$, the optimal cut may intersect intra-block edges, and thus the block's internal structure must be considered. In this case, the DAG-based model splitting algorithm is applied to determine the optimal cut. If $a_B^{min} \geq a_B^{in}$, the optimal cut does not intersect any intra-block edges, so the

block's internal structure can be abstracted. In this case, the block-wise model splitting algorithm is employed to reduce complexity while determining the optimal cut. The detailed descriptions of the block-level abstraction are provided in the following subsection.

B. Block-Level Abstraction

1) *Procedure:* To further reduce computational complexity, we leverage the structural regularity of blocks by abstracting each repeated block as a single vertex in the DAG. This simplification significantly reduces the number of vertices and edges, thereby accelerating the computation of the minimum $s-t$ cut. The detailed procedure is as follows.

Firstly, we initialize a simplified DAG denoted as $\bar{\mathcal{G}} = (\bar{\mathcal{V}} \cup \{D, S\}, \bar{\mathcal{E}})$ and set $\bar{\mathcal{V}} = \mathcal{V}$ and $\bar{\mathcal{E}} = \mathcal{E}$. Let M denote the number of blocks in $\bar{\mathcal{G}}$, and the set of blocks is indexed by $\mathbf{V}_B = [\mathcal{V}_B^1, \mathcal{V}_B^2, \dots, \mathcal{V}_B^M]$. Each block is sequentially replaced by a single vertex in $\bar{\mathcal{G}}$. Let v_B^m denote the vertex that replaces block \mathcal{V}_B^m .

Secondly, the edge weights between v_B^m and other vertices in $\bar{\mathcal{G}}$ are calculated based on the original connections of block \mathcal{V}_B^m . The weight of the edge from v_B^m to sink vertex S , denoted by $w_{(v_B^m, S)}$, is the sum of the device execution weights of all vertices within block \mathcal{V}_B^m , i.e.,

$$w_{(v_B^m, S)} = \sum_{v_b \in \mathcal{V}_B^m} w_{(v_b, S)}. \quad (19)$$

Thirdly, the weight of the edge from source vertex D to v_B^m in $\bar{\mathcal{G}}$, denoted by $w_{(D, v_B^m)}$, is the sum of the server execution weights of all vertices within this block, i.e.,

$$w_{(D, v_B^m)} = \sum_{v_b \in \mathcal{V}_B^m} w_{(D, v_b)}. \quad (20)$$

Fourthly, for any parent vertex of block \mathcal{V}_B^m , denoted as v_p , the weight of the edge from v_p to vertex v_B^m , denoted by $w_{(v_p, v_B^m)}$, is given by

$$w_{(v_p, v_B^m)} = w_{(v_p, v_b)}, \quad (21)$$

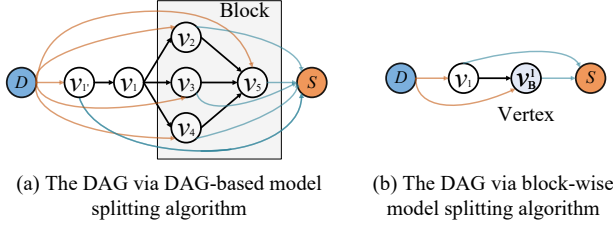


Fig. 7: An example of DAG transformation via DAG-based and block-wise model splitting algorithms.

where v_b is any vertex in block \mathcal{V}_B^m .

Fifthly, for any child vertex of block \mathcal{V}_B^m , denoted as $v_{\bar{b}}$, the weight of the edge from vertex v_B^m to vertex $v_{\bar{b}}$, denoted by $w_{(v_B^m, v_{\bar{b}})}$, is given by

$$w_{(v_B^m, v_{\bar{b}})} = \sum_{v_b \in \mathcal{V}_B^m} w_{(v_b, v_{\bar{b}})}. \quad (22)$$

The same abstraction procedure is applied to all blocks in the model.

2) *Example:* To illustrate the above transformation process more clearly, we provide an example as follows. Fig. 7(a) shows a DAG \mathcal{G}' constructed by the DAG-based model splitting algorithm, where a block is highlighted. Its corresponding DAG $\bar{\mathcal{G}}$ constructed by the block-wise model splitting algorithm, is shown in Fig. 7(b). In $\bar{\mathcal{G}}$, the entire block is replaced by a single vertex v_B^1 . The weight of the edge from this integrated vertex v_B^1 to the source vertex S , denoted as $w_{(v_B^1, S)}$, is the sum of the weights of all original edges from S to the vertices within the block:

$$w_{(v_B^1, S)} = w_{(v_2, S)} + w_{(v_3, S)} + w_{(v_4, S)} + w_{(v_5, S)}. \quad (23)$$

Similarly, the weight of the edge from the sink vertex D to v_B^1 , denoted as $w_{(D, v_B^1)}$, is the sum of the weights of all original edges from the intra-block vertices to D :

$$w_{(D, v_B^1)} = w_{(D, v_1)} + w_{(D, v_3)} + w_{(D, v_4)} + w_{(D, v_5)}. \quad (24)$$

The weight of the edge from vertex v_1 to integrated vertex v_B^1 , denoted as $w_{(v_1, v_B^1)}$, is the weight of any one of the edges from v_1 to the intra-block vertices:

$$w_{(v_1, v_B^1)} = w_{(v_1, v_2)}. \quad (25)$$

For the DAG in Fig. 7(a), there are 17 edges and 8 vertices. After the block integration by using the block-wise model splitting algorithm, there are only 5 edges and 4 vertices in the simplified DAG, as shown in Fig. 7(b). The block-wise model splitting algorithm can make the DAG a more streamlined structure, therefore reducing the computational complexity of finding the optimal cut.

C. Block-Wise Model Splitting Execution

Although the DAG is simplified through block-level abstraction, the abstracted DAG $\bar{\mathcal{G}}$ may still contain parent vertices with multiple outgoing edges. To ensure accurate cut selection, the abstracted DAG is passed to Alg. 2 to obtain the optimal

Algorithm 3: Block-Wise Model Splitting Algorithm.

```

1 Build a DAG  $\mathcal{G}$  for an AI model based on Alg. 1;
2 Calculate  $a_B^{\text{in}}$  and  $a_B^{\text{min}}$  based on the intra-block cut
  detection;
3 if  $a_B^{\text{min}} < a_B^{\text{in}}$  then
  // The optimal cut intersects
  // intra-block edges.
4 Obtain optimal cut  $c^*$  by inputting DAG  $\mathcal{G}$  into
  Algorithm 2;
5 else
  // The optimal cut does not
  // intersect any intra-block edges.
6  $\bar{\mathcal{E}} \leftarrow \mathcal{E}$ ,  $\bar{\mathcal{V}} \leftarrow \mathcal{V}$ ;
7 Identify and define the block set  $\mathbf{V}_B$ ;
8 for  $\mathcal{V}_B^m$  in  $\mathbf{V}_B$  do
9 Replace block  $\mathcal{V}_B^m$  with vertex  $v_B^m$  in  $\bar{\mathcal{V}}$ ;
10 Add edges  $(v_n, v_B^m)$ ,  $(D, v_B^m)$ ,  $(v_B^m, v_n)$ ,
    and  $(v_B^m, S)$  into  $\bar{\mathcal{E}}$ ;
11 Calculate these edge weights connected to
    vertex  $v_B^m$  based on Eqs. (19)–(22);
12 Assign edge weights to these edges;
13 end
14  $\bar{\mathcal{G}} = (\bar{\mathcal{V}} \cup \{D, S\}, \bar{\mathcal{E}})$ ;
15 Obtain optimal cut  $c^*$  by inputting DAG  $\bar{\mathcal{G}}$  into
    Algorithm 2;
16 end

```

cut. Compared to directly applying the DAG-based model splitting algorithm, the block-wise model splitting algorithm reduces the number of vertices and edges by abstracting repeated blocks, thereby lowering the computational complexity.

The overall execution of the block-wise model splitting algorithm consists of three key steps. Firstly, we determine whether an AI model contains repeated blocks. If not, the DAG-based model splitting algorithm is directly applied. If blocks are present, the block-wise model splitting algorithm is applied. Secondly, the intra-block cut identification is performed to check whether the optimal cut interacts any intra-block edges. If it does, we retain the full block structure and use the DAG-based model splitting algorithm. Otherwise, each block is abstracted as a single vertex to simplify the DAG. Thirdly, the abstracted DAG is fed into the DAG-based model splitting algorithm to determine the optimal cut. The detailed procedure of the proposed block-wise model splitting algorithm is presented in Alg. 2.

D. Computational Complexity Analysis

In our proposed model splitting algorithms, the computational complexity depends on the structure of the AI model, i.e., whether it is linear or nonlinear. For a linear AI model, the optimal cut can be directly obtained using a simple brute-force search method on the AI model, since no parent vertex has multiple outgoing edges. The computational complexity of the brute-force search method is $O(L)$, where L is the number of layers in the AI model. For a nonlinear AI model,

we represent this AI model as a DAG and solve the minimum s - t cut using a maximum flow algorithm. In this work, we adopt Dinic’s algorithm [21], which is known for its efficiency in network flow problems. The computational complexity of Dinic’s algorithm is $O(|\mathcal{V}|^2|\mathcal{E}|)$, where $|\mathcal{V}|$ is the number of vertices, and $|\mathcal{E}|$ is the number of edges in the DAG.

VII. PERFORMANCE EVALUATION

In this section, we first evaluate the performance of the proposed DAG-based and block-wise model splitting algorithms for determining the optimal cut. Then, we assess the performance of the proposed solution in wireless networks.

A. Performance of the Proposed Algorithms

1) *Simulation Setup*: In this subsection, the proposed DAG-based and block-wise model splitting algorithms are evaluated by executing them on a server to obtain the optimal cut. This server is equipped with an Intel Xeon(R) Gold 6226R CPU. The proposed splitting algorithms are compared with the following benchmarks:

- **Brute-force** [6], which exhaustively examines all possible subsets to find the optimal cut.
- **Regression** [7], which fits the quantitative relationship between the cut position and key factors in an AI model, thereby transforming the cut selection problem into a continuous optimization problem. The optimal cut is then obtained by solving this optimization problem.

Since the regression method cannot directly handle nonlinear AI models, the block-level abstraction described in Section VI-B is applied to convert the model into a linear form, enabling compatibility with the regression approach.

To compare the cuts obtained by the proposed algorithms with those from the brute-force search method, we evaluate AI models containing nonlinear blocks. However, due to the exponential computational complexity of brute-force search, applying it to complex models is impractical. Therefore, we consider three representative networks, each incorporating a single type of nonlinear block, as illustrated in Fig. 8. These blocks are: *residual blocks* [26], which introduce skip connections that add inputs directly to the outputs of convolutional layers; *inception blocks* [27], which combine multiple convolutional filters of varying kernel sizes; and *dense blocks* [28], which connect each layer to all subsequent layers to enhance feature reuse.

In addition, to evaluate the of the proposed algorithms, experiments are conducted on four widely adopted AI models with varying depths and architectural patterns: *GoogLeNet*, a 22-layer model with 9 inception blocks, an average layer output size of 22 MB, and a total computational workload of 50 GFlops; *ResNet18*, an 18-layer model with 8 residual blocks, an average layer output size of 1.1 MB, and a total computational workload of 1.8 GFlops; *ResNet50*, a 50-layer model with 16 residual blocks, an average layer output size of 1.5 MB, and a total computational workload of 3.7 GFlops; and *DenseNet121*, a 121-layer model with 58 dense blocks, an average layer output size of 29 MB, and a total computational workload of 92 GFlops.

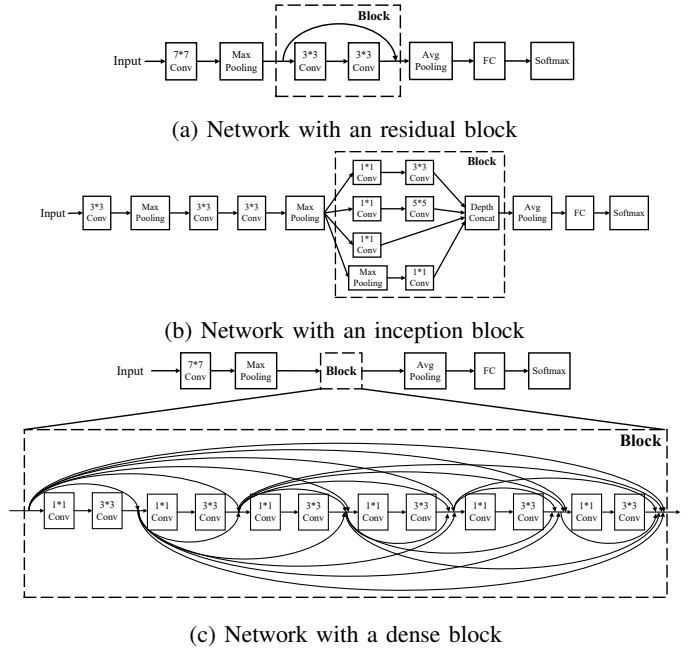


Fig. 8: The structures of networks with residual, inception, and dense blocks, which exhibit different intra-block connections.

The *running time* is defined as the time taken by the server to execute an algorithm and then identify the optimal cut for SL. The *probability of the optimal cut* refers to the probability that the cut obtained by an algorithm exactly matches the one obtained by the brute-force search method.

2) *Effectiveness of the Proposed Algorithms*: Since the regression method has a constant-time computational complexity of $\mathcal{O}(1)$, its theoretical complexity is omitted from the experimental analysis. Fig. 9(a) illustrates the computational complexity comparison between our proposed algorithms and the brute-force search method on networks with a single block. The DAG-based model splitting algorithm significantly outperforms the brute-force search method, achieving reductions in computational complexity by $1.9\times$, $143.3\times$, and $166.1\times$ for networks with residual, inception, and dense blocks, respectively. Moreover, the block-wise model splitting algorithm further streamlines the process, achieving additional complexity reductions of $3.2\times$, $4.9\times$, and $66.9\times$ over the DAG-based algorithm. This is because, in AI models with block structures, the block-wise model splitting algorithm simplifies the DAG architecture, enabling more efficient identification of the optimal cut.

Figure 9(b) presents the average probability of the optimal cut over 1,000 simulation runs on networks with a single block. Although the regression method has the lowest computational complexity, it suffers from a low probability of the optimal cut. For example, on the networks with residual and dense blocks, the probability is only 73.6%. In particular, its probability drops to zero on the network with an inception block. This is because the regression method fails to accurately capture the relationship between the split point and model parameters, particularly the size of the smashed data. In contrast, our proposed algorithms obtain the optimal cut across

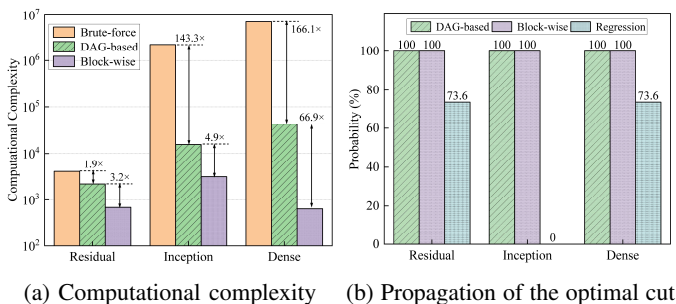


Fig. 9: Performance comparison among the proposed algorithms and benchmarks on networks with a single block.

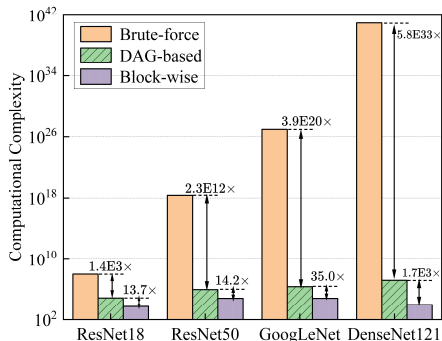


Fig. 10: Computational complexity comparison among the proposed algorithms and benchmarks on different AI models.

all three network types. This is because the cuts are optimal by the proposed algorithms, which is proved in Theorem 1.

Figure 10 presents the computational complexity of three algorithms on different AI models. It can be seen that the DAG-based model splitting algorithm significantly reduces computational complexity compared to the brute-force search method, while the block-wise model splitting algorithm further reduces the computational complexity compared to the DAG-based model splitting algorithm. Specifically, for DenseNet121, the DAG-based model splitting algorithm achieves a 5.8×10^{33} reduction in computational complexity compared to the brute-force search method. The block-wise model splitting algorithm further reduces the complexity by an additional factor of 1.7×10^3 compared to the DAG-based model splitting algorithm. That is because DenseNet121 contains the highest number of repeated blocks among these models.

3) *Running Time of the Proposed Algorithms*: We evaluate the running time of the proposed algorithms on both networks with a single block and full AI models. Due to the high complexity of full AI models, we only measure the running time of the brute-force search method on simpler block-based networks. All experimental results are averaged over 1,000 simulation runs to ensure statistical reliability.

Figure 11(a) compares the running time of the proposed algorithms against two baselines on the block-based networks. The DAG-based model splitting algorithm reduces the running time by 12.1 \times , 4,015.6 \times , and 9,998.4 \times across the three networks, respectively, compared to the brute-force search method. Furthermore, the block-wise model splitting algorithm achieves additional reductions of 1.2 \times , 1.9 \times , and 3.1 \times com-

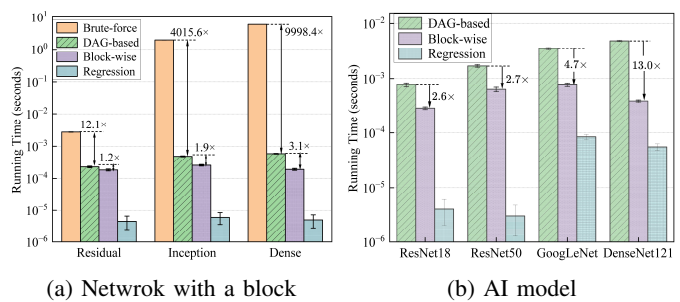


Fig. 11: Running time comparison among the proposed algorithms and benchmarks.

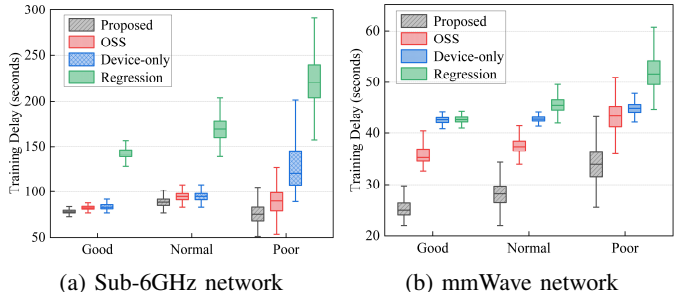


Fig. 12: Training delay per epoch among the proposed solution and benchmarks when training GoogLeNet.

pared to the DAG-based model splitting algorithm.

Figure 11(b) presents the running time of the proposed algorithms on four full AI models. The results show that the block-wise model splitting algorithm consistently achieves lower running time than the DAG-based model splitting algorithm across all AI models. Although the regression method achieves the lowest running time overall, it fails to identify the optimal cut, resulting in significantly higher training delay. The limitations of the regression method will be presented in the following subsection.

B. Proposed Scheme Performance in Dynamic Edge Networks

1) *Simulation Setup*: We evaluate the proposed algorithms using a custom designed edge network simulator. The simulator's key components are provided as follows.

Network Topology: The proposed solution is tested in two representative edge network environments: mmWave and sub-6GHz networks. Each edge network consists of a single base station equipped with a server and connected to 20 mobile devices via wireless links. For wireless data transmission, the n257 band is used in the mmWave network, and the n1 band is used in the sub-6GHz network, following 3GPP specifications [29], [30].

Device Mobility: These devices located within the base station's coverage area request access and begin the device-side model training task at the start of each experimental trial. Each device continues to run the task while the devices move along a pre-defined trajectory at a speed of 30 km/h. The link bitrate is converted by new radio channel quality indicator to modulation and coding scheme mapping table [31]. Although the channel and link scheme does not account

TABLE I
TRAINING DELAY COMPARISON AMONG DIFFERENT SCHEMES

Model	Method	Training Delay (minutes)			
		CIFAR-10		CIFAR-100	
		IID (Accuracy 95%)	non-IID (Accuracy 95%)	IID (Accuracy 79 ± 1%)	non-IID (Accuracy 78 ± 1%)
GoogLeNet	OSS	2,872.04 (1.33 ×)	3,839.34 (1.33 ×)	3,201.44 (1.29 ×)	3,601.12 (1.29 ×)
	Device-only	3,265.28 (1.51 ×)	4,367.28 (1.51 ×)	3,851.60 (1.55 ×)	4,105.14 (1.54 ×)
	Regression	3,489.76 (1.61 ×)	4,737.32 (1.64 ×)	3,911.03 (1.57 ×)	4,390.73 (1.65 ×)
	Proposed	2,164.36	2,891.81	2,489.61	2,660.29
ResNet18	OSS	2,905.48 (1.28 ×)	3,272.18 (1.29 ×)	3,127.26 (1.25 ×)	3,327.46 (1.34 ×)
	Device-only	3,331.11 (1.47 ×)	3,640.04 (1.43 ×)	3,407.30 (1.36 ×)	3,361.40 (1.35 ×)
	Regression	3,201.30 (1.41 ×)	3,502.76 (1.38 ×)	3,440.95 (1.38 ×)	3,318.70 (1.34 ×)
	Proposed	2,265.09	2,540.26	2,499.24	2,484.79
ResNet50	OSS	3,242.20 (1.33 ×)	4,208.29 (1.16 ×)	2,790.26 (1.28 ×)	3,842.83 (1.36 ×)
	Device-only	3,685.03 (1.51 ×)	5,586.54 (1.56 ×)	3,187.27 (1.46 ×)	4,057.17 (1.55 ×)
	Regression	3,639.25 (1.49 ×)	5,490.38 (1.52 ×)	3,113.14 (1.43 ×)	4,038.32 (1.43 ×)
	Proposed	2,445.16	3,611.98	2,179.92	2,819.09
DenseNet121	OSS	3,717.68 (1.16 ×)	4,215.98 (1.15 ×)	3,002.23 (1.28 ×)	4,300.22 (1.33 ×)
	Device-only	4,940.63 (1.55 ×)	5,744.91 (1.57 ×)	3,420.54 (1.46 ×)	5,021.96 (1.55 ×)
	Regression	4,921.35 (1.54 ×)	5,702.53 (1.56 ×)	3,374.06 (1.44 ×)	4,954.29 (1.53 ×)
	Proposed	3,196.94	3,652.77	2,341.60	3,232.60

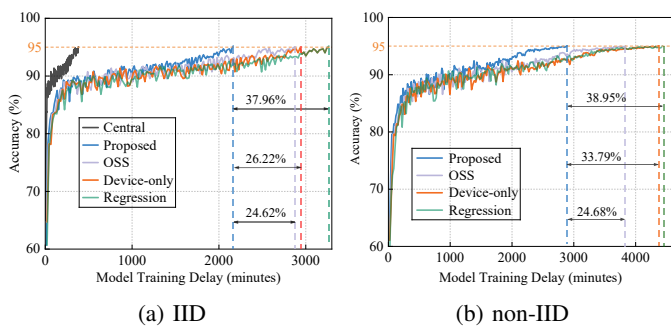


Fig. 13: Overall training delay comparison among the proposed solution and benchmarks when training GoogLeNet.

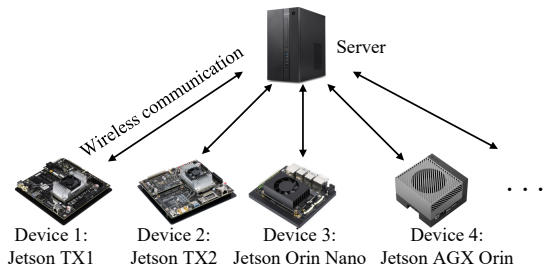


Fig. 14: Prototype system of SL.

for complex propagation effects, it effectively simulates real-world mobile cellular dynamics, making it suitable for testing model splitting.

Channel Condition: Taking directional antenna gain into account, the transmit power is calculated as $P = P_e - 10 \log_{10} N$, where P_e is the average effective isotropically radiated power (EIRP), and N is the number of beams. The average EIRP of the server is fixed at 40 dBm for sub-6GHz networks and 50 dBm for mmWave networks [32]. The number of beams is set to 16 and 64 for sub-6GHz and mmWave networks, respectively. The large-scale path loss is

represented as

$$PL(dB) = 32.5 + 20 \log_{10}(f) + 10\eta \log_{10}(d) + \chi, \quad (26)$$

where f , η , d , and χ represent the carrier frequency, path-loss exponent, transmission distance, and shadow fading, respectively. The shadow fading follows $\mathcal{N}(0, \sigma^2)$. In this paper, the channel condition is set to three states: *Good*, *Normal*, and *Poor*, corresponding to σ values of 2 dB, 4 dB, and 6 dB, respectively.

Computation Delay Profiles: To accurately measure computation delay, develop a standalone Python-based latency profiling tool for *PyTorch*. This tool traverses the AI model and registers forward and backward hooks on each layer, following the method introduced in [33]. These hooks record per-layer processing times during training, enabling fine-grained profiling of training delays. For communication delay estimation, we use *PyTorch*'s built-in `torchstat` module to record each layer's parameter size and output size. All training and profiling experiments are performed on graphics processing units (GPUs).

Our prototype system is illustrated in Fig. 14, consisting of a server and 20 devices configured as follows: (i) a personal computer (pc) with 1× Nvidia RTX A6000 GPU; (ii) five Jetson TX1, each with 256-core Nvidia Maxwell GPU; (iii) five Jetson TX2, each with 256-core Nvidia Pascal GPU; (iv) five Jetson Orin Nano, each with 1024-core Nvidia Ampere architecture GPU; and (v) five Jetson AGX Orin, each with 2048-core Nvidia Ampere architecture GPU. Through the prototype system, we measure training delay profiles on both the server and heterogeneous mobile devices, demonstrating the system's ability to adapt to real-world variations in device capabilities. The performance of the proposed solution is compared with three benchmarks:

- **Optimal static splitting (OSS)** [13], which represents the best static cut among all possible static cuts, where the cut layer splitting the AI model remains fixed throughout the experiment.

- **Device-only**, where the entire AI model is trained on the device, while the server is only responsible for data transmission.
- **Regression** [7], as mentioned in the previous subsection.

2) *Impact of Channel Conditions*: To evaluate the performance of the proposed solution under dynamic wireless environments, we train GoogLeNet over 300 simulation runs across three channel conditions.

Figure 12 illustrates the model training delay per epoch for each method under both sub-6GHz and mmWave networks. The regression method performs poorly due to its suboptimal cut. In contrast, the proposed solution consistently achieves the lowest training delay across all channel conditions. In the sub-6GHz network, the proposed solution reduces training delay by 11.40%, 40.14%, and 65.69% compared to the OSS, device-only, and regression methods, respectively. In the mmWave network, the proposed solution also outperforms all benchmarks, achieving training delay reductions of 31.65%, 32.56%, and 37.54%, respectively. These results demonstrate that the proposed solution can rapidly determine the optimal cut based on real-time network conditions, especially in highly dynamic environments.

3) *Impact of Data Distribution*: To evaluate the performance of the proposed solution under different data distributions, we train GoogLeNet and compare it against four benchmarks: *central*, which runs the entire model on the server, *OSS*, *device-only*, and *regression*. The experiments are conducted in the mmWave network with normal channel conditions. Two types of data distributions are considered, i.e., independent and identically distributed (IID) and non-IID. In the IID setting, each device receives an equal number of samples from each class in the dataset. In this experiment, training delay is defined as the time required for the model to reach 95% accuracy under each algorithm. As shown in Fig. 13(a), the proposed solution reduces the training delay by 37.96%, 26.22%, and 24.62% compared to the regression, device-only, and OSS benchmarks, respectively.

In the non-IID dataset, we employ the method described in [34] to synthesize data for different devices. Specifically, each device samples data from a subset of categories, where the category proportions $\mathcal{Q} = q_1, q_2, \dots, q_M$ follow a Dirichlet distribution, i.e., $\mathcal{Q} \sim \text{Dir}(\gamma p)$. Here, p represents the label distribution, and γ controls the degree of data heterogeneity across devices. In this experiment, we set $\gamma = 0.5$. As shown in Fig. 13(b), the proposed solution reduces the training delay by 38.95%, 33.79%, and 24.68% compared with the regression, device-only, and OSS benchmarks, respectively. This demonstrates that under non-IID data conditions, the proposed solution exhibits more pronounced advantages, which highlights its robustness to heterogeneous data distributions.

4) *Impact of AI Models*: All models are trained over the mmWave network with normal channel conditions. To ensure a fair comparison, all schemes are required to achieve their predefined accuracy thresholds using the same datasets, data distributions, and AI models. These thresholds may vary slightly across models due to inherent differences in their performance. For example, on the CIFAR-100 dataset with a non-IID data distribution and using ResNet18, the accuracy

threshold is set at 77%, while for ResNet50 under the same conditions, the threshold is 78%.

The overall training delay for each method to reach its accuracy threshold is summarized in Table I. It can be seen that the proposed solution substantially reduces training delay compared with benchmarks across all AI models, datasets, and data distributions. For example, when training DenseNet121 on the CIFAR-100 dataset with a non-IID data distribution, the proposed solution reduces the overall training delays by 1.33 \times , 1.55 \times , and 1.53 \times compared with the OSS, device-only, and regression methods, respectively. These performance gains are primarily attributed to the proposed solution's ability to select the optimal cut that minimizes the overall training delay, thereby mitigating resource bottlenecks and accelerating the overall training process.

VIII. CONCLUSION

In this paper, we have investigated the model splitting problem for SL over dynamic edge networks. We have represented the AI model as a DAG and then proposed a DAG-based model splitting algorithm, which is proved to be optimal. In addition, we have proposed a block-wise model splitting algorithm for AI models with block structures, which reduces the computational complexity of obtaining optimal cut selection. Extensive experimental results have validated that the proposed solution can make the optimal model splitting for SL in real time. Due to its capability of handling arbitrary AI model architectures, the proposed scheme provides a general solution for deploying AI models over resource-constrained edge networks. For the future work, we will investigate efficient model splitting schemes for complicated large language models.

APPENDIX

A. Proof of Theorem 1

For a block, let $T(c_B^{\min})$ and $T(c_B^{\text{in}})$ denote the total training delay under cut values a_B^{\min} and a_B^{in} , respectively. The difference between them is given by

$$T(c_B^{\min}) - T(c_B^{\text{in}}) = N \frac{a_B^{\min} - a_B^{\text{in}}}{R_D} + N \frac{a_B^{\min} - a_B^{\text{in}}}{R_S} + \frac{\sum_{i \in \mathcal{V}_B} k_{v_i}}{R_D} + \frac{\sum_{i \in \mathcal{V}_B} k_{v_i}}{R_S} + \sum_{i \in \mathcal{V}_B} N (\xi_{D,v_i} - \xi_{S,v_i}), \quad (\text{A.1})$$

where \mathcal{V}_B is the set of layers within the block that are assigned to the device after the minimum s - t cut. In the right-hand side of Eq. (A.1), the first term is the difference in transmission delay for the smashed data. The second term is the difference in transmission delay for the gradient. Note that the gradient size during AI model training is equivalent to the size of smashed data. The third and fourth terms are the differences in transmission delay for the device-side model uploading and downloading, respectively. The fifth term is the difference in computation delay for processing the layers. If $a_B^{\min} \geq a_B^{\text{in}}$, we have $T(c_B^{\min}) - T(c_B^{\text{in}}) > 0$. Hence, the minimum s - t cut in the block is not optimal, and the optimal cut does not intersect any intra-block edges.

REFERENCES

- [1] S. Wang, Y. Ruan, Y. Tu, S. Wagle, C. G. Brinton, and C. Joe-Wong, "Network-aware optimization of distributed learning for fog computing," *IEEE/ACM Trans. Netw.*, vol. 29, no. 5, pp. 2019–2032, Oct. 2021.
- [2] K. B. Letaief, Y. Shi, J. Lu, and J. Lu, "Edge artificial intelligence for 6G: Vision, enabling technologies, and applications," *IEEE J. Sel. Areas Commun.*, vol. 40, no. 1, pp. 5–36, Jan. 2022.
- [3] X. Shen, J. Gao, W. Wu, M. Li, C. Zhou, and W. Zhuang, "Holistic network virtualization and pervasive network intelligence for 6G," *IEEE Commun. Surveys Tuts.*, vol. 24, no. 1, pp. 1–30, Dec. 2022.
- [4] O. Gupta and R. Raskar, "Distributed learning of deep neural network over multiple agents," *J. Netw. Comput. Appl.*, vol. 116, pp. 1–8, Aug. 2018.
- [5] J. Sun, C. Wu, S. Mumtaz, J. Tao, M. Cao, M. Wang, and V. Frascolla, "An efficient privacy-aware split learning framework for satellite communications," *IEEE J. Sel. Areas Commun.*, vol. 42, no. 12, pp. 3355–3365, Dec. 2024.
- [6] Z. Lin, G. Zhu, Y. Deng, X. Chen, Y. Gao, K. Huang, and Y. Fang, "Efficient parallel split learning over resource-constrained wireless edge networks," *IEEE Trans. Mobile Comput.*, vol. 23, no. 10, pp. 9224–9239, Oct. 2024.
- [7] Y. Wen, G. Zhang, K. Wang, and K. Yang, "Training latency minimization for model-splitting allowed federated edge learning," *IEEE Trans. Netw. Sci. Eng.*, vol. 12, no. 3, pp. 2081–2092, May 2025.
- [8] J. Li, W. Liang, Y. Li, Z. Xu, X. Jia, and S. Guo, "Throughput maximization of delay-aware DNN inference in edge computing by exploring DNN model partitioning and inference parallelism," *IEEE Trans. Mobile Comput.*, vol. 22, no. 5, pp. 3017–3030, May 2023.
- [9] 3GPP, "5G System (5GS); Study on traffic characteristics and performance requirements for AI/ML model transfer," document TR 22.874 V18.2.0, 2021.
- [10] V. Ninkovic, D. Vukobratovic, D. Miskovic, and M. Zennaro, "COM-SPLIT: A communication-aware split learning design for heterogeneous IoT platforms," *IEEE Internet Things J.*, vol. 12, no. 5, pp. 5305–5319, Mar. 2024.
- [11] J. Yan, S. Bi, and Y.-J. A. Zhang, "Optimal model placement and online model splitting for device-edge co-inference," *IEEE Wireless Commun.*, vol. 21, no. 10, pp. 8354–8367, Oct. 2022.
- [12] W. Wu, M. Li, K. Q. Qu, C. Zhou, X. Shen, W. Zhuang, X. Li, and W. Shi, "Split learning over wireless networks: Parallel design and resource management," *IEEE J. Sel. Areas Commun.*, vol. 41, no. 4, pp. 1051–1066, Apr. 2023.
- [13] C. Xu, J. Li, Y. Liu, Y. Ling, and M. Wen, "Accelerating split federated learning over wireless communication networks," *IEEE Trans. Wireless Commun.*, vol. 23, no. 6, pp. 5587–5599, Jun. 2024.
- [14] J. Dachille, C. Huang, and X. Liu, "The impact of cut layer selection in split federated learning," *arXiv:2412.15536*, 2024.
- [15] J. Lee, J. Cho, W. Lee, M. Seif, and H. V. Poor, "Game-theoretic joint incentive and cut layer selection mechanism in split federated learning," *arXiv:2412.07813*, 2024.
- [16] Y. Duan and J. Wu, "Joint optimization of DNN partition and scheduling for mobile cloud computing," in *Proc. ACM ICPP*, New York, NY, USA, Oct. 2021, pp. 1–10.
- [17] H. Liang, Q. Sang, C. Hu, D. Cheng, X. Zhou, D. Wang, W. Bao, and Y. Wang, "DNN surgery: Accelerating DNN inference on the edge through layer partitioning," *IEEE Trans. Cloud Comput.*, vol. 11, no. 3, pp. 3111–3125, Jul. 2023.
- [18] Y. Dai, L. Lyu, N. Cheng, M. Sheng, J. Liu, X. Wang, S. Cui, L. Cai, and X. Shen, "A survey of graph-based resource management in wireless networks - part II: Learning approaches," *IEEE Trans. Cogn. Commun. Netw.*, 2024, DOI:10.1109/TCCN.2024.3508777.
- [19] L. Wu, G. Gao, J. Yu, F. Zhou, Y. Yang, and T. Wang, "PDD: Partitioning DAG-topology DNNs for streaming tasks," *IEEE Internet Things J.*, vol. 11, no. 6, pp. 9258–9268, Mar. 2024.
- [20] Y. Kang, J. Hauswald, C. Gao, A. Rovinski, T. Mudge, J. Mars, and L. Tang, "Neurosurgeon: Collaborative intelligence between the cloud and mobile edge," *ACM SIGARCH Comput. Archit. News*, vol. 45, no. 1, pp. 615–629, Apr. 2017.
- [21] Y. Dinitz, *Dinitz' Algorithm: The Original Version and Even's Version*. Berlin, Heidelberg: Springer Berlin Heidelberg, 2006, pp. 218–240. [Online]. Available: https://doi.org/10.1007/11685654_10
- [22] C. Szegedy, W. Liu, Y. Jia, P. Sermanet, S. Reed, D. Anguelov, D. Erhan, V. Vanhoucke, and A. Rabinovich, "Going deeper with convolutions," in *Proc. IEEE CVPR*, Boston, Massachusetts, USA, Jun. 2015, pp. 1–9.
- [23] K. He, X. Zhang, S. Ren, and J. Sun, "Deep residual learning for image recognition," in *Proc. IEEE CVPR*, Las Vegas, Nevada, USA, Jun. 2016, pp. 770–778.
- [24] G. Huang, Z. Liu, L. Van Der Maaten, and K. Q. Weinberger, "Densely connected convolutional networks," in *Proc. IEEE CVPR*, Honolulu, Hawaii, USA, Jul. 2017, pp. 4700–4708.
- [25] M. Stoer and F. Wagner, "A simple min cut algorithm," in *Proc. Eur. Symp. Algorithms*, Sep. 1994, pp. 141–147.
- [26] S. Targ, D. Almeida, and K. Lyman, "ResNet in ResNet: Generalizing residual architectures," *arXiv:1603.08029*, 2016.
- [27] C. Szegedy, S. Ioffe, V. Vanhoucke, and A. Alemi, "Inception-v4, Inception-ResNet and the impact of residual connections on learning," in *Proc. AAAI*, Palo Alto, USA, Feb. 2017, pp. 4278–4284.
- [28] G. Huang, S. Liu, L. Van der Maaten, and K. Q. Weinberger, "CondenseNet: An efficient DenseNet using learned group convolutions," in *Proc. IEEE CVPR*, Salt Lake City, Utah, USA, Jun. 2018, pp. 2752–2761.
- [29] 3GPP, "NR; User equipment (UE) radio transmission and reception," document TS 38.101-1 V18.6.0, 2024.
- [30] M. L. Hakim, M. T. Islam, and T. Alam, "Incident angle stable broadband conformal mm-Wave FSS for 5G (n257, n258, n260, and n261) band EMI shielding application," *IEEE Antennas Wirel. Propag. Lett.*, vol. 23, no. 2, pp. 488–492, Feb. 2024.
- [31] 3GPP, "NR; Physical layer procedures for data," document TS 38.214 V17.3.0, 2022.
- [32] Y. Wang, X. Chen, and X. Chu, "Performance analysis for hybrid Sub-6GHz-mmWave-THz networks with downlink and uplink decoupled cell association," *IEEE Trans. Wireless Commun.*, 2025, DOI:10.1109/TWC.2025.3555114.
- [33] S. Wang, X. Zhang, H. Uchiyama, and H. Matsuda, "HiveMind: Towards cellular native machine learning model splitting," *IEEE J. Sel. Areas Commun.*, vol. 40, no. 2, pp. 626–640, Feb. 2022.
- [34] C. Feng, H. H. Yang, D. Hu, Z. Zhao, T. Q. Quek, and G. Min, "Mobility-aware cluster federated learning in hierarchical wireless networks," *IEEE Trans. Wireless Commun.*, vol. 21, no. 10, pp. 8441–8458, Oct. 2022.